0026-895X/06/6903-776–787$20.00
MOLECULAR PHARMACOLOGY
Vol. 69, No. 3
16873/3084528
Mol Pharmacol 69:776–787, 2006
Printed in U.S.A.

Identification of Zebrafish ARNT1 Homologs: 2,3,7,8-Tetrachlorodibenzo-*p*-dioxin Toxicity in the Developing Zebrafish Requires ARNT1

Amy L. Prasch, Robert L. Tanguay, Vatsal Mehta, Warren Heideman, and Richard E. Peterson

School of Pharmacy (W.H., R.E.P.) and Molecular and Environmental Toxicology Center (A.L.P., V.M., W.H., R.E.P.), University of Wisconsin, Madison, Wisconsin; and Department of Environmental and Molecular Toxicology, Oregon State University, Corvallis, Oregon (R.L.T.)

Received July 19, 2005; accepted November 9, 2005

ABSTRACT

To use the zebrafish (*Danio rerio*) as a model to study 2,3,7,8-tetrachlorodibenzo-*p*-dioxin (TCDD) developmental toxicity, it is essential to know which proteins are involved in mediating toxicity. Previous work has identified zfAHR2 as the receptor that binds TCDD mediating downstream responses. Although zfARNT2b can form a functional heterodimer with zfAHR2 in vitro, *zfarnt2* null mutants show no protection against endpoints of TCDD developmental toxicity, demonstrating that zfARNT2b cannot be the physiological dimerization partner for zfAHR2 mediating responses to TCDD in zebrafish embryos. The purpose of the current study was to identify an alternate dimerization partner(s) for zfAHR2 that may function to mediate TCDD developmental toxicity. By searching zebrafish genomic sequence and using the polymerase chain reaction-based rapid amplification of cDNA ends technique, three forms of cDNA that seem to be alternate mRNA splice variants of a zebrafish homolog of ARNT1 were detected. Analysis of the zfARNT1 proteins in vitro demonstrates that the two longest forms of zfARNT1, zfARNT1b and zfARNT1c, can form functional heterodimers with zfAHR2. However, the shortest form, zfARNT1a, seems to be nonfunctional with zfAHR2 in vitro. To determine whether a zfARNT1 protein functions with zfAHR2 in vivo, a morpholino targeted against the 5′ end of zfARNT1 (*zfarnt1*-MO) was used. Injection of the *zfarnt1*-MO before TCDD treatment significantly decreases the induction of zfCYP1A mRNA and protein. In addition, *zfarnt1* morphants show complete protection against TCDD-induced pericardial edema and show partial protection against reduced blood flow and craniofacial malformations caused by TCDD, demonstrating the role of zfARNT1 proteins in mediating these responses.

Polychlorinated dibenzo-*p*-dioxins are lipophilic, persistent, bioaccumulative toxicants. Developing fish are among the most sensitive species to the toxicity of these compounds (Peterson et al., 1993) and 2,3,7,8-tetrachlorodibenzo-*p*-dioxin (TCDD), the most potent polychlorinated dibenzo-*p*-dioxin, has adversely affected feral fish populations of lake trout (*Salvelinus namaycush*), the most sensitive fish species to TCDD developmental toxicity (Cook et al., 2003). However, the mechanism by which TCDD causes adverse effects on fish development is unclear. The zebrafish (*Danio rerio*) makes an attractive model in which to study the developmental toxicity of TCDD because of their rapid growth, high egg yield, short generation time, and rapid, external development. In addition, their developmental biology has been well characterized, the zebrafish genome is near completion, and numerous molecular and genetic techniques have been developed to study gene function. Finally, the zebrafish displays a similar set of endpoints of toxicity upon TCDD exposure as other freshwater fish species, including pericardial edema, arrested growth, craniofacial malformations, ischemia, anemia, impaired swim bladder inflation, and mortality (for review, see Tanguay et al., 2003).

Studies of aryl hydrocarbon receptor $(AHR)^{-/-}$ mouse lines

This work was supported by the University of Wisconsin Sea Grant College Program, National Oceanic and Atmospheric Administration, U.S. Department of Commerce, Sea Grant Project Numbers R/BT-16 and R/BT-17 (to W.H. and R.E.P.). This research was also supported by National Institutes of Health/National Institute of Environmental Health Sciences grants T32-ES07015 and R01-ES0127716 (to W.H. and R.E.P) and R01-ES10820, ES00210, and ES03850 (to R.L.T).

Article, publication date, and citation information can be found at http://molpharm.aspetjournals.org.

doi:10.1124/mol.105.016873.

ABBREVIATIONS: TCDD, 2,3,7,8-tetrachlorodibenzo-*p*-dioxin; AHR/ahr, aryl hydrocarbon receptor; ARNT, aryl hydrocarbon receptor nuclear translocator; XRE, xenobiotic response element; hpf, hour(s) postfertilization; zfARNT, zebrafish aryl hydrocarbon receptor nuclear translocator; PCR, polymerase chain reaction; bp, base pair(s); RACE, rapid amplification of cDNA ends; MO, morpholino; wt, wild type, mut, mutant; CMV, cytomegalovirus; ANOVA, analysis of variance; bHLH, basic helix loop helix; MS-222, ethyl 3-aminobenzoate methanesulfonate.

have clearly demonstrated the role of the AHR signaling pathway in mediating responses to TCDD (Fernandez-Salguero et al., 1996; Mimura et al., 1997), and signaling through the AHR has been well characterized in mammals (for review, see Schmidt and Bradfield, 1996). To use zebrafish as a model to study TCDD developmental toxicity, it was essential to identify and characterize the zebrafish AHR signaling pathway, and much is now known about its components. Three forms of the AHR (zfAHR1, zfAHR1B, and zfAHR2) have been identified in zebrafish (Tanguay et al., 1999; Andreasen et al., 2002a; Karchner et al., 2005), and morpholino knockdown of zfAHR2 has identified it as the receptor that binds TCDD, leading to downstream effects (Prasch et al., 2003; Teraoka et al., 2003; Dong et al., 2004). In untreated zebrafish liver cells, zfAHR2 has been shown to shuttle between the cytoplasm and nucleus. However, upon treatment with the ligand β-naphthoflavone, zfAHR2 translocates to the nucleus (Wentworth et al., 2004) where it then presumably dimerizes with an aryl hydrocarbon receptor nuclear translocator (ARNT) protein. The zfAHR2-ARNT heterodimer can then bind to xenobiotic response elements (XREs) in target genes such as *zfcyp1a*, leading to altered gene expression (Tanguay et al., 1999). Duplicate aryl hydrocarbon receptor repressor genes, zfAHRR1 and zfAHRR2, have also been identified in zebrafish (Evans et al., 2005). These proteins can negatively regulate zfAHR2 signaling in vitro, although their in vivo role in zfAHR2 biology remains unclear.

The initial ARNT protein identified in zebrafish was zfARNT2 (Tanguay et al., 2000; Wang et al., 2000). ZfARNT2 exists as multiple splice forms, one form of which, zfARNT2b, can form a functional heterodimer in vitro with zfAHR2 that can specifically recognize XREs in DNA binding assays and induce XRE-driven transcription in COS-7 cells incubated with TCDD (Tanguay et al., 2000). ZfAHR2, zfARNT2a,b,c, and zfCYP1A mRNAs have also been shown to colocalize in tissues of the cardiovascular system after TCDD exposure (Andreasen et al., 2002b). These data suggested that zfARNT2b was the likely dimerization partner for zfAHR2 in vivo involved in mediating responses to TCDD. However, analysis of *zfarnt2* morphant and *zfarnt2*$^{-/-}$ mutant embryos has demonstrated that zfARNT2 is not essential for the development of endpoints of TCDD toxicity, because both *zfarnt2* morphants and null mutants show similar sensitivity to TCDD as wild-type embryos (Prasch et al., 2004b).

The sensitivity of the zfARNT2-deficient fish to TCDD toxicity suggested that an alternate form(s) of ARNT must exist in the zebrafish embryo that functionally dimerizes with zfAHR2. The purpose of this work was to identify and characterize this putative ARNT in zebrafish and to determine its role in mediating TCDD developmental toxicity. Indeed, three novel cDNAs that encode proteins with sequence similarity to rainbow trout (*Oncorhynchus mykiss*) ARNT and mammalian ARNT1—zfARNT1a, zfARNT1b, and zfARNT1c—were identified. In vitro analysis of these proteins demonstrates that two forms, zfARNT1b and zfARNT1c, can form functional heterodimers with zfAHR2, and in vivo morpholino antisense knockdown experiments demonstrate an essential role for zfARNT1 proteins in mediating several TCDD-dependent endpoints in developing zebrafish.

Materials and Methods

Oligonucleotides. Oligonucleotides used for PCR and gel shift reactions were synthesized by Integrated DNA Technologies (Coralville, IA) and are written 5′ to 3′. The predicted initiation ATG codon is indicated in bold, and the sequence encoding the BamHI restriction site in the ARNTF2bam primer is lowercase. For the gel shift oligonucleotides, the XRE core consensus sequence is underlined and mutated bases are in bold. PCR oligonucleotides: ARNTF1, ATCCTGCGCATGGCCGTATC; ARNTR1, GATGTAGCCTGTGCAGTGGAC; SRARNTR1,AACCACATACTGCTGCTCGCCGTCTTT; SRARNTF1,TCAGAGAGCAGCTTTCCACCACCGAGAA; SRARNTF2, CCGGATGTTGGATATGAAAACGGGCAC; ARNTF2bam, ggatccCTTTGCCTGTCGGAC**ATG**ACA; ARNTF2, CTTTGCCTGTCGGAC**ATG**ACA; ARNTR2, GAACATATCCCTCAGCTCTTCTTAATG; ARNTR3, AGGACACGGTGTAAGACTAC; ARNTR4, ACAAAAGGGCAAAATAGGTCC. Gel shift oligonuceotides: wtXREF, GGCTCTTCTCACGCAACTCCGG; wtXRER, GCCCCGGAGTTGCGTGAGAAGA; mutXREF, GGCTCTTCTC**G**CGCAACTCCGG; mutXRER, GCCCCGGAGTTGCG**C**GAGAAGA.

ZfARNT1 Identification and Cloning. Primers ARNTF1 and ARNTR1 were initially used to amplify a portion of zfARNT1 sequence identified in the Ensembl release of the zebrafish genome. The single amplified 550-bp product was subcloned into pGEM-T Easy vector (Promega, Madison, WI) and sequenced. A PCR-based approach was then used to identify the 5′ and 3′ ends of zfARNT1 using the SMART RACE cDNA amplification kit (Clontech, Mountain View, CA) as described by the manufacturer. One microgram of the poly(A) RNA generated from 72-hpf zebrafish embryos was reversed transcribed using PowerScript reverse transcriptase with either the 5′-CDS primer and SMART 11 A oligo (5′ RACE-ready cDNA) or the 3′ CDS primer (3′ RACE-ready cDNA). PCR reactions were performed using 2.5 μl of each RACE-ready cDNA as a template with the SRARNTR1 or SRARNTF1 gene specific primers and the supplied universal primer. The 3′ RACE reaction was reamplified using the SRARNTF2 nested primer and the supplied nested universal primer. A single 5′ RACE product and two distinct 3′ RACE products were amplified, subcloned into pGEM-T Easy vector, and sequenced. The 5′ RACE product showed high sequence similarity to other forms of ARNT1 and contained a likely translational start site; however, both 3′ RACE products were truncated compared with ARNT1s from other species and did not seem to encode the full-length 3′ end of ARNT1. A clone from the Sangre Center (Cambridge, UK) was subsequently identified (GenBank accession number BX927222) as containing the genomic sequence for zfARNT1. Analysis of this genomic clone revealed additional 3′ sequences with similarity to ARNT1 of other species.

cDNA Constructs for Functional Studies. Because all putative forms of zfARNT1 contained the same 5′ end, the same forward primer (ARNTF2) was used to amplify each form. The zfARNT1a and zfARNT1b sequences were amplified using the ARNTF2 primer containing an additional BAMH1 sequence on the 5′ end (ARNTF2bam). ZfARNT1a was amplified using the ARNTR3 reverse primer, zfARNT1b was amplified using the ARNTR2 reverse primer, and zfARNT1c was amplified using the ARNTR4 reverse primer. To obtain full-length transcripts, zfARNT1a and zfARNT1b were amplified out of cDNA generated using SuperScript II reverse transcriptase (Invitrogen, Carlsbad, CA) from 500 ng of poly(A) RNA that had been isolated from whole 72-hpf embryos. PCR was performed on this cDNA using high-fidelity PfuTurbo polymerase (Stratagene, La Jolla, CA). Adenines were added to the amplified products before cloning into pGEM-T Easy and sequencing. The full-length zfARNT1c was amplified from an adult fin cDNA library using high-fidelity KOD polymerase (EMD Biosciences, San Diego, CA), subcloned into PCRII TOPO Blunt vector (Invitrogen), and sequenced. To generate expression vectors for zfARNT1a and zfARNT1b, inserts were excised from pGEM-T Easy by digestion with BamHI (site included in ARNTF2 primer) and NotI and cloned into pBKCMV

(Stratagene) previously cut with the same enzymes to generate pBKCMV-zfARNT1a and pBKCMV-zfARNT1b. The pBKCMV-zfARNT1c expression vector was generated by excising the insert from the PCRII TOPO vector with EcoRI digest and inserting into the EcoRI site of pBKCMV.

Nucleotide and Amino Acid Sequence Analysis. Both strands of each clone were sequenced at least three times using fluorescent dye-labeling cycle sequencing (Applied Biosystems, Foster City, CA; University of Wisconsin Biotech Center, Madison, WI; Oregon State University, Center for Gene Research and Biotechnology, Corvallis, OR) stepwise using gene-specific primers before GenBank submission. The Baylor College of Medicine Human Genome Center (Houston, TX) search launcher, the National Center for Biotechnology Information, and Vector NTI software (Invitrogen) were used for sequence analysis.

Comparative Analysis of zfARNT1 and zfARNT2 mRNA Abundance. RNA was isolated from pools of 10 vehicle-exposed embryos and extracted using the RNeasy mini kit (QIAGEN, Valencia, CA) according to the manufacturer's instructions. cDNA was produced from 750 ng of each total RNA sample using SuperScript II (Invitrogen) and oligo(dT) primer in 20 μl. The LightCycler (Roche Diagnostics, Indianapolis, IN) was used for quantitative real-time PCR. To compare expression levels of zfARNT1 and zfARNT2, relative quantitation software (Roche Diagnostics) was used to perform calibrator normalized relative quantification using efficiency correction. Target genes (zfARNT1 and zfARNT2) and a reference loading control gene (β-actin) were amplified in triplicate for each sample. The ARNTF1 and ARNTR1 primer set was used to amplify all splice forms of zfARNT1. Primers used to amplify zfARNT2b/c and β-actin were described previously (Andreasen et al., 2002b). Efficiencies for each primer set were determined from amplifications with standard curves and are included in the calculation of the expression value for each gene. The expression of the target and reference genes were also determined in a calibrator (cDNA from whole adult tissue) that is included in each light cycler run to control for run-to-run variability. To get the final abundance values for zfARNT1, the zfARNT1/β-actin ratio was calculated for each sample and normalized to the ARNT1/β-actin ratio obtained in the adult cDNA sample. Likewise, the normalized ratio of ARNT2/β-actin was also determined in each sample to compare the relative abundance of these two transcripts.

In Vitro Transcription and Translation. In vitro transcription and translation of zfAHR2, zfARNT2b, zfARNT1a, zfARNT1b, and zfARNT1c proteins was performed using the TNT-coupled rabbit reticulocyte lysate system (Promega). Recombinant proteins were expressed from pBKCMV expression constructs described here and by Tanguay et al. (1999, 2000) with T3 polymerase as described by the manufacturer. For in vitro DNA binding assays, each protein was expressed alone or zfAHR2 was coexpressed with either zfARNT2b, zfARNT1a, zfARNT1b, or zfARNT1c in the presence of 10 nM TCDD or vehicle (dimethyl sulfoxide). Side reactions containing [^{35}S]methionine were performed to assess relative protein production. To test the *zfarnt1*-MO, 12.5-μl reactions were performed using 250 ng of template DNA, 1.5 μl of [^{35}S]methionine, and either no morpholino or 500 nM final concentration of control-MO or *zfarnt1*-MO. After 90-min incubation at 30°C, radioactive translation products were resolved by 8% polyacrylamide gel electrophoresis, dried, and PhosphorImaged (Molecular Dynamics, Sunnyvale, CA).

In Vitro DNA Binding Assay. Double-stranded probes were made by annealing the forward and reverse oligonucleotides for the wild-type (wt) and mutant (mut) XRE. Annealing was performed by combining 0.5 nmol of each oligonucleotide in 0.1 M NaCl and 0.01 M Tris, pH 8.0, heating to 70°C for 10 min, and then cooling to room temperature. Double-stranded probes were radiolabeled with [^{32}P]dCTP using the Prime-a-Gene kit (Promega). The gel shift was performed by combining the in vitro-synthesized protein mixtures with binding buffer (20 mM HEPES, pH 8.0, 100 mM NaCl, 1 mM dithiothreitol, and 6% glycerol), 2 μg of poly(dI-dC), 15 fmol of radiolabeled wtXRE, and a 10-fold molar excess of unlabeled wtXRE or mutXRE competitor DNAs when indicated. After a 15-min incubation at room temperature, complexes were resolved on a 0.5× Tris borate-EDTA (90 mM Tris, 64.6 mM boric acid, and 2.5 mM EDTA, pH 8.3) and 4% acrylamide gel. The dried gel was exposed to a phosphor screen for 2 days.

Transient Transactivation Assay. COS-7 cells were plated on 24-well plates at a density of 8×10^4 cells/well 1 day before transfection, which was performed using SuperFect (QIAGEN). Each well was cotransfected with 400 μl of serum-containing media containing pBKCMV expression constructs for zfAHR2, zfARNT1a, zfARNT1b, zfARNT1c, or zfARNT2b (450 ng), *prt1aluc* luciferase reporter construct (100 ng), and β-galactosidase CMV reporter (50 ng) as indicated. After a 2.5-h incubation at 37°C, the transfection mixture was removed and replaced with 1 ml of serum-containing media. After 22.5-h incubation, each well was exposed to either dimethyl sulfoxide (vehicle) or 10 nM TCDD and incubated for another 20 h. Luciferase assay was performed using the Luciferase assay system (Promega) and a ML-2250 luminometer (Dynatech Labs, Chantilly, VA). One hundred microliters of lysis buffer was added to each well, and after a 15-min incubation a 10-μl aliquot of cell lysate was transferred to a luminometer plate. For the luciferase assay, 50 μl of luciferase assay buffer was injected into each well, a 2-s incubation was performed, and luminescence was integrated over 10 s. Transfection efficiency was determined by measuring the β-galactosidase activity for each well. Thirty microliters of cell lysate was aliquoted into a 96-well plate followed by the addition of 200 μl of reaction buffer (0.1 M $NaPO_4$, 10 mM KCl, 1 mM $MgCl_2$, and 0.385% β-mercaptoethanol) and 40 μl of 4 mg/ml *o*-nitrophenyl-β-D-galactopyranoside. The reaction was incubated for 3 h at 37°C, and plates were read at 405 nM using an ELx800 plate reader (Bio-Tek Instruments, Winooski, VT).

Antisense Morpholinos. The zebrafish arnt1 morpholino (*zfarnt1*-MO) obtained from Gene Tools (Philomath, OR) was designed with sequence complementary to the zfARNT1 cDNA. The *zfarnt1*-MO overlapped the first predicted translation start site of zfARNT1 mRNA by starting 8 bp upstream of the predicted AUG start codon and continuing to 14 bp downstream. The sequence of the *zfarnt1*-MO was 5′-GGATTAGCTGATGTCATGTCCGACA-3′, and it was fluorescein tagged at the 3′ end to monitor injection success. The standard control morpholino sold by Gene Tools (5′-CTCTTACCTCAGTTACAATTTATA-3′) was used as the control morpholino (control-MO). Before embryo injection, morpholinos were diluted to 0.12 mM in 1× Danieau's solution [58 mM NaCl, 0.7 mM KCl, 0.4 mM $MgSO_4$, 0.6 mM $Ca(NO_3)_2$, and 5 mM HEPES, pH 7.6] as described by Nasevicius and Ekker (2000).

Microinjection and Waterborne TCDD Exposure of Zebrafish Embryos. Fertilized eggs were obtained from adult AB strain zebrafish bred in our laboratory as described by Westerfield (1995). Embryos were raised at a water temperature of 27°C; water was changed daily; and when appropriate, embryos were euthanized with tricaine (1.67 mg/ml MS-222; Sigma-Aldrich, St. Louis, MO).

For microinjection, newly fertilized eggs were injected with either the *zfarnt1* or control-MO at the one- to two-cell stage with approximately 13 ng of the morpholino. Embryos were allowed to develop for 2 h, after which unfertilized and damaged eggs were discarded. Viable *zfarnt1*-MO-injected embryos (*zfarnt1* morphants) were observed for fluorescence as an index of injection success demonstrated by uniform distribution of the morpholino. Only *zfarnt1*-MO injected embryos exhibiting fluorescence were used.

Waterborne exposure of embryos to TCDD occurred from approximately 3 to 4 hpf. TCDD of >99% purity obtained from Chemsyn (Lenexa, KS) was dissolved in dimethyl sulfoxide. Embryos from each injection group (uninjected, control-MO injected, or *zfarnt1*-MO injected) were exposed to vehicle (0.1% dimethyl sulfoxide) or TCDD (0.4 ng/ml) for 1 h in glass scintillation vials with gentle rocking. After the 1-h static exposure, embryos were rinsed with water and maintained in vehicle/TCDD-free water for the remainder of experiments.

Analysis of zfCYP1A mRNA Abundance. To analyze zfCYP1A mRNA abundance, RNA was isolated from pools of 15 vehicle and TCDD-exposed embryos from each injection group (uninjected, control-MO injected, and *zfarnt1*-MO injected; n = pool of 15). cDNA was prepared as described above, and quantitative real-time PCR for zfCYP1A and β-actin was performed as described previously (Andreasen et al., 2002b; Prasch et al., 2003).

Whole Mount Immunolocalization of zfCYP1A. Embryos were anesthetized at 72 hpf and fixed in 4% paraformaldehyde in phosphate-buffered saline. Tissue-specific expression of zfCYP1A was determined using the monoclonal antibody Mab1-12-3 (Park et al., 1986) as described previously (Andreasen et al., 2002b; Prasch et al., 2003; Carney et al., 2004).

Assessment of TCDD Developmental Toxicity in zfarnt1 Morphants. Vehicle- and TCDD-exposed embryos from each injection group were assessed for three endpoints of TCDD toxicity: pericardial edema, reduced peripheral blood flow, and reduction in lower jaw growth. All were measured as described previously (Prasch et al., 2003; Carney et al., 2004). Pericardial edema was measured at 72 and 96 hpf by photographing embryos in a lateral orientation and quantitating the area of the pericardial sac using Scion Image for Windows (Scion Corporation, Frederick, MD). The result obtained for the vehicle-exposed uninjected group was subtracted from all other treatment groups to obtain an increase in pericardial area because of edema. As an index of regional blood flow, peripheral red blood cell perfusion rates were measured at 72, 96, and 120 hpf by counting the number of red blood cells passing through an intersegmental vein in the posterior quarter of the trunk during a 7.5-s period using time-lapse recording. To determine the extent of reduced lower jaw growth, the distance between the anterior edge of the lower jaw and the anterior edge of the eye was measured. This lower jaw-to-eye gap was measured from digital photographs of embryos mounted in lateral orientation at 96 hpf. Using Scion Image, a straight vertical line was first drawn along the anterior edge of the eye. A second straight horizontal line was then drawn from the anterior edge of the lower jaw to intersect the vertical line. Length of the horizontal line was the measure of lower jaw-to-eye gap. If the lower jaw had grown to extend in front of the eye, the measure was given a negative value. If the lower jaw remained behind the eye, the measure was given a positive value.

Statistical Analysis. Significance was determined using a factorial ANOVA followed by the Fisher's least significant difference test. Levene's test for homogeneity of variances was performed before the ANOVA. Data sets that did not pass Levene's test were transformed by $\log_{10}$ transformation (COS-7 cell assay, zfCYP1A mRNA abundance) or square root transformation (red blood cell perfusion rate), and the transformed data were analyzed by the factorial ANOVA. Repeated attempts at transforming the pericardial edema data to pass Levene's test were unsuccessful; therefore, significance was determined for appropriate comparisons using a pairwise t test assuming unequal variances. All statistical analysis was performed using the Statistica 6.0 software package (StatSoft, Tulsa, OK). Results are presented as mean $\pm$ S.E.; level of significance was $p \leq 0.05$.

Results

Identification of zfARNT1 cDNAs. Using a combination of BLAST searching and PCR-based RACE technique, three distinct forms of zfARNT1 were identified. A single 1.1-kilobase product was obtained in the 5′ RACE reaction, and the nested 3′ RACE reaction yielded two distinct products of 0.9 and 1.2 kilobases, both of which contained in frame stop codons. Both 3′ RACE products were truncated compared with other known ARNT1 proteins, suggesting that an additional full-length form of ARNT1 went undetected in the 3′ RACE reactions. To identify additional 3′ ARNT1 sequence, zebrafish genomic sequence was again BLAST searched. A clone from the Sanger Centre (GenBank accession number BX927222) was identified as containing the genomic sequence for zfARNT1. This genomic clone contained the entire sequence identified in the 5′ and 3′ RACE reactions and also contained additional 3′ sequence that was similar to ARNT1 of other species. Analysis of this genomic clone sequence and the RACE reactions has lead to the identification of three distinct mRNA splice variants for zfARNT1: zfARNT1a, zfARNT1b, and zfARNT1c. These transcripts share the same putative translation initiation site but diverge on the 3′ end to generate three distinct transcripts.

To amplify the predicted open reading frames, a common forward primer that included the predicted ATG (ARNTF2 or ARNTF2bam) and three different reverse primers (ARNTR2, ARNTR3, and ARNTR4) were used. A 1301-bp product was obtained using the ARNTF2bam/ARNTR3 primer set, which we have named zfARNT1a. A 1544-bp product was obtained with the ARNTF2bam/ARNTR2 primer set, which we have named zfARNT1b, and a 2199-bp product was obtained with the ARNTF2/ARNTR4 primer set, which we have named zfARNT1c. The zfARNT1c transcript was originally amplified from an adult fin cDNA library but has subsequently been detected in cDNA generated from 72-hpf embryos. The zfARNT1a sequence encodes a 404-amino acid protein with a theoretical molecular mass of 44 kDa, the zfARNT1b sequence encodes a 503-amino acid protein with a theoretical molecular mass of 56 kDa, and the zfARNT1c sequence encodes a 728-amino acid protein with a theoretical molecular mass of 79 kDa. The nucleotide sequences for zfARNT1a, zfARNT1b, and zfARNT1c have been deposited in the GenBank database under accession numbers AY707650, AY707649, and DQ140179, respectively.

Phylogenetic analysis was used to determine the relationship of the newly identified zebrafish protein sequences to ARNT protein sequences of other species (Fig. 1). This result demonstrates that the identified proteins are in fact members of the vertebrate ARNT clade. It is noteworthy that the

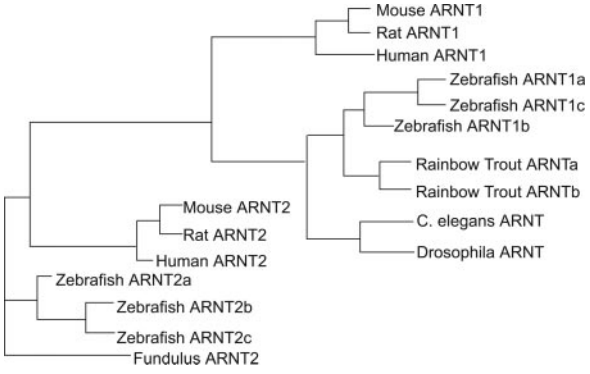

Fig. 1. Phylogenetic analysis of ARNT proteins. Using Vector NTI software, the amino acid sequences of various ARNT proteins were aligned using Align X alignment program, and this alignment was used to construct the phylogenetic tree using the neighbor joining method. The GenBank accession numbers for the ARNT sequences used are as follow: *Homo sapiens* (human) ARNT1, BC060838 and ARNT2, BC036099; *Mus musculus* (mouse) ARNT1, BC012870 and ARNT2, BC054546; *Rattus norvegicus* (rat) ARNT1, U61184 and ARNT2, U61405; zebrafish ARNT2a, AF219987; ARNT2b, AF219988; ARNT2c, AF219989; ARNT1a, AY707650; ARNT1b, AY707649; and ARNT1c; DQ140179; *Fundulus heteroclitus* (fundulus) ARNT2, AF079311; rainbow trout ARNTa, U73840 and ARNTb, U73841; *Drosophila melanogaster* ARNT, AF154417; and *Caenorhabditis elegans* ARNT, NM060286.

protein sequences are most closely related to ARNT1 proteins of other species and are distinct from the mammalian and fish ARNT2 proteins, providing evidence that a zebrafish homolog of ARNT1 has been identified.

Although it is possible that these three zfARNT1 cDNAs arise from separate genes, it seems more likely that they are the result of alternate splicing of mRNA from the same gene. Sequence comparisons demonstrate that the zfARNT1a, zfARNT1b, and zfARNT1c proteins are identical over the first 390 amino acids and share significant homology with the previously cloned zfARNT2 proteins in this region (Fig. 2). All three zfARNT1 proteins contain the highly conserved

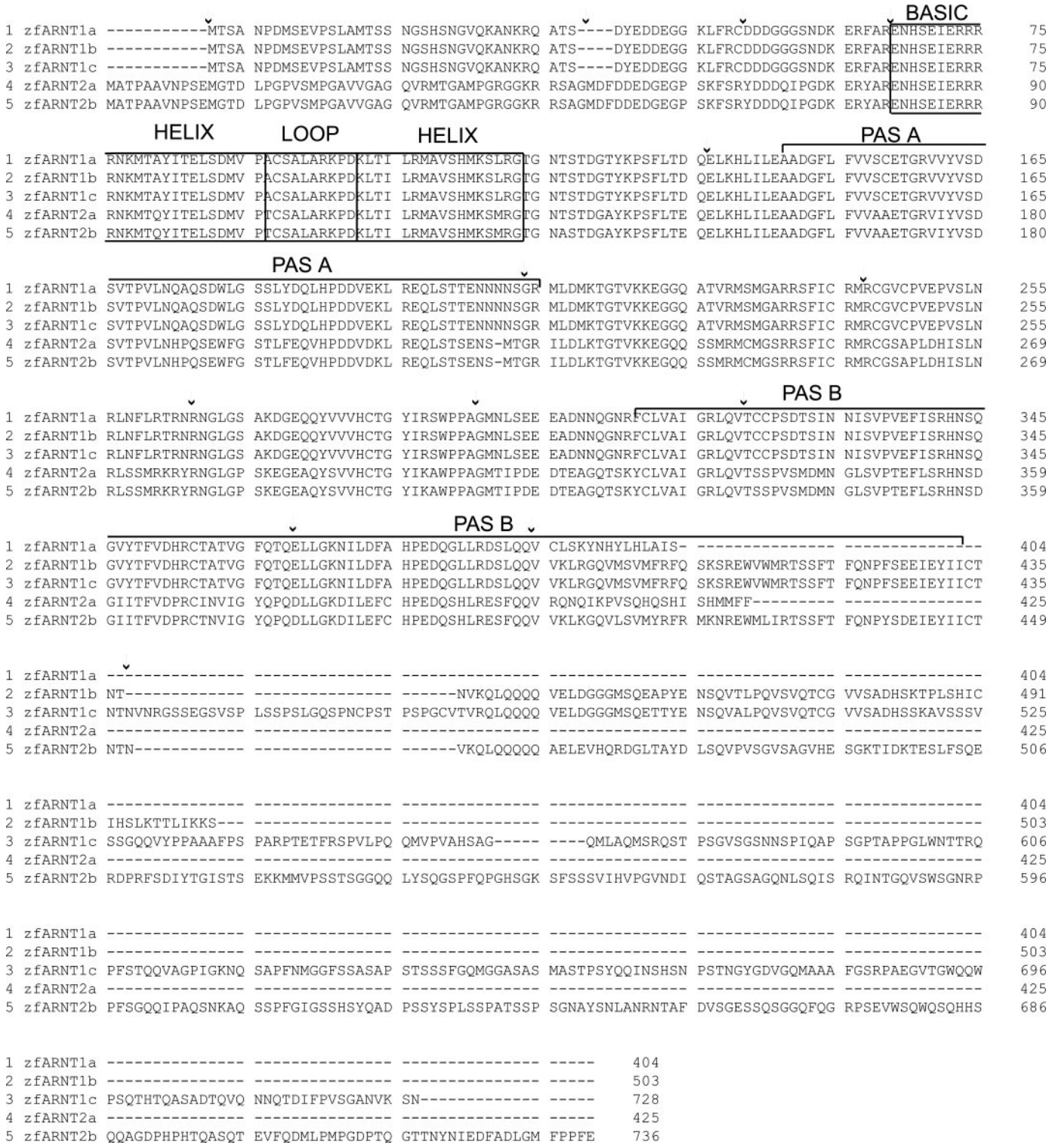

Fig. 2. Amino acid sequence alignment of the predicted zfARNT1a, zfARNT1b, and zfARNT1c sequences with zfARNT2a and zfARNT2b. Sequence alignment was performed using the ClustalW 1.8 alignment program (http://www.ebi.ac.uk/clustalw/). Alignment gaps are represented by dashes. The regions encoding the conserved bHLH, PAS A, and PAS B domains are indicated. The position of predicted exon-exon boundaries derived from the mouse ARNT1 exon-exon boundaries and also from information available in the Ensembl release of the zebrafish genome are indicated by arrows.

basic helix loop helix (bHLH) and PAS A domains that are known to be important for DNA binding and heterodimerization. The zfARNT1a sequence contains a portion of the PAS B domain but diverges within this domain and truncates with 14 unique amino acids. This divergence occurs at a site predicted as an intron-exon boundary. Alternate splicing at the same position occurs to form the zfARNT2a protein (Fig. 2). The zfARNT1b sequence contains the entire PAS B domain and continues for an additional 64 amino acids before terminating to create a protein that is shorter than other ARNTs lacking the C-terminal domain found in other ARNT proteins (Li et al., 1994; Pollenz et al., 1996; Tanguay et al., 2000). The zfARNT1c protein is similar in length to other known mammalian and fish ARNT proteins containing complete bHLH, PAS A, and PAS B domains and also containing a full-length C-terminal domain with sequence similarity to the C-terminal domains of previously identified mammalian and fish ARNT proteins (Li et al., 1994; Pollenz et al., 1996; Tanguay et al., 2000).

In Vitro Expression of zfARNT1a and zfARNT1b and in Vitro DNA Binding. As an initial step in characterizing the properties of the zfARNT1 proteins, zfARNT1a, zfARNT1b, and zfARNT1c were produced in vitro from pBKCMV expression constructs using an in vitro-coupled transcription/translation system. As predicted, the approximate size of the zfARNT1a protein was 44 kDa, the zfARNT1b protein was 56 kDa, and the zfARNT1c protein was 79 kDa (Fig. 3A).

To determine whether the zfARNT1 proteins are able to form a functional complex with zfAHR2, DNA binding ability was determined in vitro. ZfARNT2b was included in this experiment for purposes of comparison. For these experiments, the zfARNT proteins were produced individually in the presence of TCDD (Fig. 3A, lanes 1–5) or together with

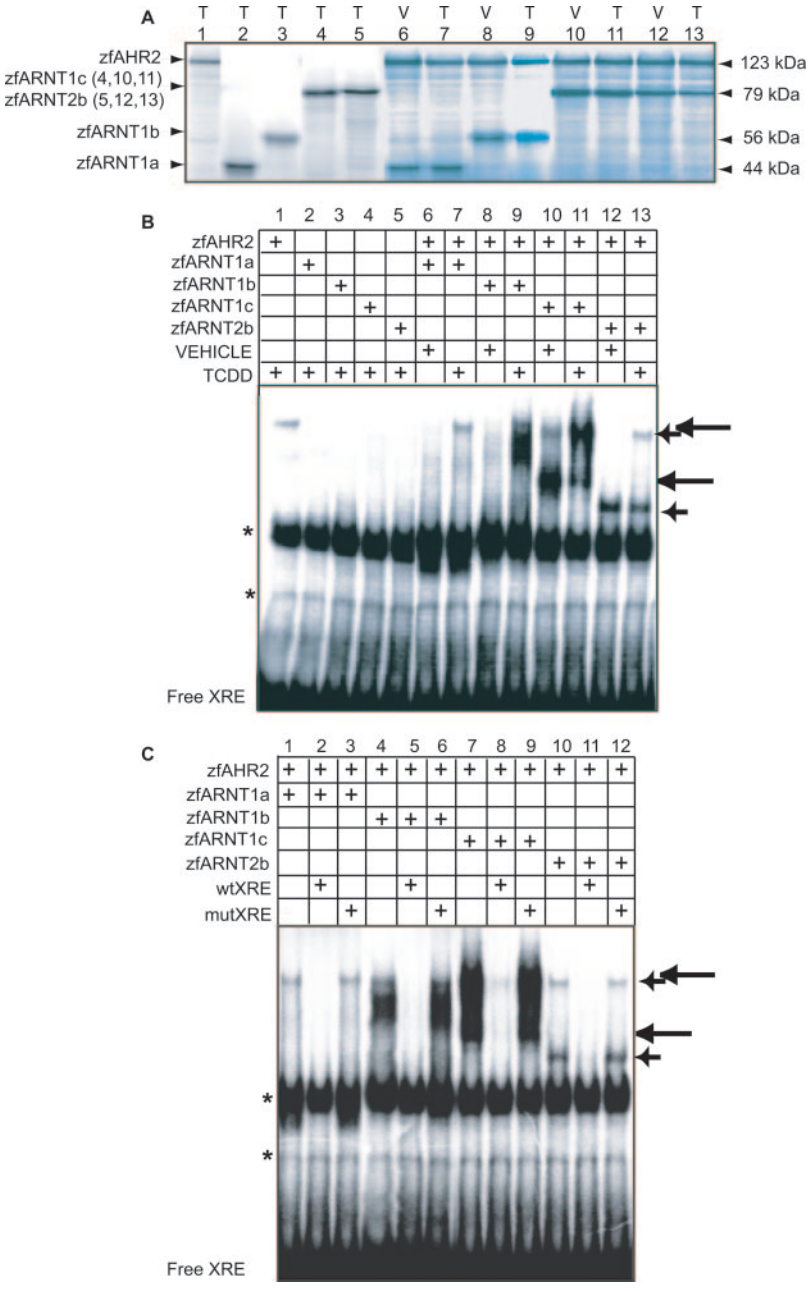

Fig. 3. In vitro translation and gel shift analysis to determine interactions between zfAHR2, zfARNT1a, zfARNT1b, zfARNT1c, and an XRE in response to TCDD exposure. A, proteins used in the gel shift analysis were synthesized in vitro either alone or in combination with zfAHR2 in the presence of either vehicle (V) or 10 nM TCDD (T). A subfraction of the protein was expressed with [^{35}S]methionine, resolved on an 8% SDS polyacrylamide gel, and the dried gel was PhosphorImaged. B, in vitro-translated proteins, either alone or in combination, were incubated in the presence of ^{32}P-labeled DNA probes containing an XRE from the mouse *cyp1a* enhancer in the presence or absence of TCDD as indicated. C, ZfAHR2 and the indicated zfARNT protein were incubated with the ^{32}P-labeled DNA probe and a 10-fold molar excess of unlabeled probe containing wtXRE or mutXRE in the presence of TCDD as indicated. The two long arrows indicate specific interactions that occur between zfAHR2 and zfARNT1c. The two shorter arrows indicate specific interactions that occur between zfAHR2 and zfARNT2b. Asterisks indicate nonspecific lysate-derived bands.

zfAHR2 in the presence of vehicle or TCDD (Fig. 3A, lanes 6–13), and their ability to bind to a radiolabeled probe containing an XRE sequence from the mouse *cyp1a* promoter was determined. None of the proteins when expressed individually in the presence of TCDD showed significant ability to bind XRE sequences, although nonspecific lysate derived bands were detected (Fig. 3B, lanes 1–5). The zfARNT1a/zfAHR2 heterodimer did not bind XRE sequences in the absence of TCDD and showed only weak ability to bind XRE sequences upon TCDD exposure (Fig. 3B, lanes 6 and 7). The zfARNT1b/zfAHR2 heterodimer also lacked ability to bind XRE in the absence of TCDD; however, upon TCDD exposure a significant shift in the labeled XRE probe was observed (Fig. 3B, lanes 8 and 9). The zfARNT1c/zfAHR2 heterodimer showed the greatest ability to interact with the XRE sequence. A complex with the XRE was observed even in the absence of TCDD (Fig. 3B, lane 10), and formation of this complex was enhanced upon TCDD exposure (Fig. 3B, lane 11). The zfARNT2b/zfAHR2 heterodimer also showed the ability to interact with zfAHR2 to bind XRE sequences as has been reported previously (Fig. 3B, lanes 12 and 13) (Tanguay et al., 2000), but this interaction seems less robust than that observed with zfARNT1b and zfARNT1c. The differential ability to bind DNA cannot be explained by different levels of protein abundance, because [^{35}S]methionine sublabeling demonstrates that each reaction contains similar levels of proteins (Fig. 3A), and the proteins have similar numbers of methionine residues. Instead, this suggests that there are likely to be structural and functional differences between the proteins that affect their ability to interact with zfAHR2 and XRE sequences. As has been reported previously (Tanguay et al., 2000; Andreasen et al., 2002a), this complex migrates as two distinct shifted bands, although the nature of this doublet is still unclear.

To demonstrate the specificity of the interactions, gel shifts were performed in the presence of unlabeled wtXRE or mutXRE oligomer probes (Fig. 3C). The complexes formed by zfAHR2 and each of the zfARNT proteins could be competed by addition of a 10-fold molar excess of unlabeled wtXRE (Fig. 3C, lanes 2, 5, 8, and 11). However, when the mutXRE that contained a single base pair change in the core XRE sequence was added, no competition with the radiolabeled probe was observed (Fig. 3B, lanes 3, 6, 9, and 12).

Transactivation Activity of zfAHR2 and zfARNT1 in COS-7 Cells. Because zfARNT1b and zfARNT1c have the ability to interact with zfAHR2 and bind XRE sequences, it was necessary to determine whether zfAHR2/zfARNT1b/c heterodimers could function to promote transcription of the luciferase reporter gene under control of an XRE-containing promoter. COS-7 cells were transiently transfected with expression constructs for zfAHR2, zfARNT2b, zfARNT1a, zfARNT1b, or zfARNT1c individually or in combinations along with the *prt1aluc* luciferase reporter construct, which contains a portion of the rainbow trout cyp1a promoter driving luciferase expression as described previously (Tanguay et al., 1999; Fig. 4). Individual transfections of all constructs resulted in low basal levels of reporter activity and no inducibility upon TCDD exposure. Consistent with its weak ability to bind DNA, zfARNT1a showed very little ability to promote transactivation of the XRE-containing reporter construct. However, when either zfARNT1b or zfARNT1c were cotransfected with zfAHR2, the basal level of reporter activity was elevated, and with both proteins there was a significant induction of reporter activity upon exposure to TCDD. As reported previously (Tanguay et al., 2000), cotransfection of zfAHR2 and zfARNT2b also caused elevation of both basal and TCDD-induced levels of reporter activity. However, both the basal and TCDD-induced levels observed with zfARNT2b were lower than those with zfARNT1b or zfARNT1c, suggesting that zfARNT2b is less able to promote transactivation on the XRE-containing promoter than the zfARNT1 proteins. However, because protein levels in COS-7 cells were not assessed, it is possible that the observed differences were because of differential ARNT protein expression levels with each transfection.

Developmental Expression of zfARNT1 and zfARNT2. The temporal expression pattern of zfARNT1a,b,c was examined using quantitative real-time PCR with gene-specific primers that amplified all spice variants of zfARNT1 (Fig. 5). Pools of vehicle-exposed embryos were collected at 24, 48, 72, and 96 hpf, and the relative abundance of zfARNT1a,b,c mRNA was determined. ZfARNT1a,b,c expression was detectable at 24 hpf and remained unchanged through 48 hpf. Between 48 and 72 hpf, expression levels in the whole embryo increased approximately 3-fold, peaking at 72 hpf, followed by a slight decrease between 72 and 96 hpf. TCDD exposure (0.4 ng/ml) did not significantly change the level of zfARNT1a,b,c expression at any time point (data not shown). These results demonstrate that zfARNT1a,b,c mRNA is expressed in the whole embryo during the period of development when TCDD toxicity occurs. It was also of interest to determine how levels of zfARNT1 mRNAs compare with levels of zfARNT2. The relative quantification software (Roche Diagnostics) was used to compare the expression level of these two genes. As can be seen in Fig. 5, zfARNT2b/c is expressed at much higher levels than zfARNT1 at all time points analyzed.

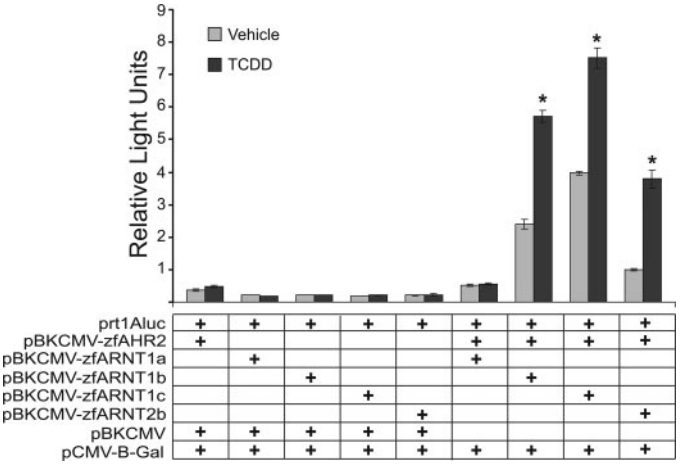

Fig. 4. Transactivation ability of zfARNT1 and zfARNT2 proteins with zfAHR2 in COS-7 cells exposed to TCDD. Cells were transiently transfected with pBKCMV expression constructs for zfAHR2, zfARNT2b, zfARNT1a, zfARNT1b, zfARNT1c; the prt1A*luc* reporter construct containing the luciferase gene under control of the rainbow trout *cyp1a* promoter and enhancer; and a β-galactosidase reporter construct as indicated. Twenty-two hours after transfection, cells were exposed to vehicle or 10 nM TCDD for 20 h and then collected for luciferase and β-galactosidase assays. Columns represent relative light units normalized to β-galactosidase activity and are mean $\pm$ S.E. of $n = 6$. $*$, significant difference between vehicle and TCDD ($p \leq 0.05$).

Morpholino Knockdown of zfARNT1. An antisense morpholino designed against the predicted start site of zfARNT1 (*zfarnt1*-MO) provides a method of transiently blocking translation of zfARNT1 proteins in the early zebrafish embryo, creating *zfarnt1* morphants, to determine whether a zfARNT1 protein is a component of the zfAHR2 signaling pathway mediating TCDD developmental toxicity. Because no antibody is currently available to detect zfARNT1 proteins, in vivo analysis of the effectiveness of the *zfarnt1*-MO was not possible. However, in vitro transcription and translation experiments demonstrate that the *zfarnt1*-MO is functional at blocking translation of zfARNT1 proteins. Results are shown for zfARNT1a as a representative zfARNT1 protein (Fig. 6). When zfARNT1a cDNA was used in the absence of morpholino, a 44-kDa protein was produced (Fig. 6, lane 1). Addition of the control-MO did not affect protein production (Fig. 6, lane 2). However, addition of *zfarnt1*-MO to the reaction decreased the production of the protein (Fig. 6, lane 3), demonstrating that the morpholino is effective at blocking translation of zfARNT1a in vitro.

A molecular marker of zfAHR2 pathway activation, zfCYP1A mRNA induction, was examined in a time-course study of *zfarnt1* morphants (Fig. 7). TCDD and vehicle-exposed embryos that were either uninjected or injected with the control-MO or *zfarnt1*-MO were used for quantitative real-time PCR of the zfCYP1A message, and its relative abundance was determined in the whole embryo. At 24 hpf, uninjected TCDD-exposed embryos had approximately a 10-fold induction of zfCYP1A mRNA compared with vehicle-exposed embryos. Injection of the control-MO did not affect this induction. However, TCDD-exposed *zfarnt1* morphants showed no induction of zfCYP1A compared with vehicle-exposed fish at 24 hpf, demonstrating an essential role for a zfARNT1 protein in mediating this induction.

The effect of the *zfarnt1*-MO on zfCYP1A induction was examined at later times to determine how long zfAHR2 signaling was decreased in the *zfarnt1* morphants. At 48 and 72 hpf, TCDD caused a further induction of the zfCYP1A message in both uninjected and control morphant embryos, reaching levels that were approximately 50-fold higher than those measured in vehicle-exposed embryos. At both time points, the *zfarnt1* morpholino continued to afford protection against zfCYP1A induction with only a 13-fold induction above vehicle observed at 48 hpf and a 17-fold induction at 72 hpf. With time, the effectiveness of the *zfarnt1*-MO decreased, and by 96 hpf no significant difference in zfCYP1A induction was observed between the uninjected, control morphant and *zfarnt1* morphant embryos that had been exposed to TCDD. Low level constitutive expression of zfCYP1A was observed in vehicle-exposed embryos at all times (relative abundance of approximately 1.5). The *zfarnt1*-MO had no effect on constitutive zfCYP1A expression at any time, suggesting that zfARNT1 proteins may not be involved in regulating constitutive levels of the zfCYP1A message.

To determine whether zfCYP1A protein induction throughout the entire embryo requires zfARNT1, whole mount immunolocalization of zfCYP1A was performed using the Mab1-12-3 antibody (Fig. 8). Results show representative staining performed at 72 hpf for vehicle-exposed embryos (top), uninjected TCDD-exposed embryos (middle), and TCDD-exposed *zfarnt1*-morphants (bottom). The left shows staining in trunk, and the right shows staining in head. As has been reported previously (Andreasen et al., 2002b), TCDD exposure results in significant zfCYP1A induction in the intersegmental veins and arteries, caudal vasculature of the trunk, vessels throughout the brain, anal and urinary pores, heart, and structures of the lower jaw. TCDD-exposed *zfarnt1* morphants show reduced zfCYP1A immunofluorescence in all of these tissues, demonstrating that zfARNT1

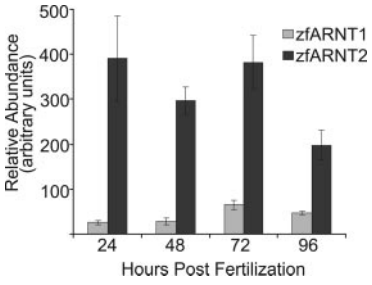

Fig. 5. Time course of zfARNT1a,b,c and zfARNT2b/c mRNA abundance. Quantitative real-time PCR was performed on cDNA using gene-specific primer sets that detected zfARNT1a,b,c, zfARNT2b/c, and β-actin. Samples were run concurrently with standard curves derived from plasmid cDNA dilutions. Relative quantification software (Roche Diagnostics) was used to compare the expression level of the zfARNT1 and zfARNT2 transcripts. RNA was extracted from pools of 10 vehicle-exposed embryos at each time (n = pool of 10 embryos). Values are mean ± S.E. of n = 4 pools.

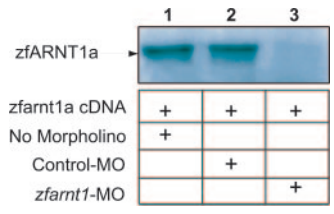

Fig. 6. Effect of the *zfarnt1*-MO on in vitro translation of the zfARNT1a protein. To determine effectiveness of the *zfarnt1*-MO at blocking translation of zfARNT1 proteins, zfARNT1 cDNAs were transcribed and translated in vitro in the presence of [^{35}S]methionine. Results are shown for zfARNT1a as a representative zfARNT1 protein. The in vitro translation reaction was performed either in the absence of morpholino (lane 1) or in the presence of the control-MO (lane 2) or *zfarnt1*-MO (lane 3). Both morpholinos were used at a final concentration of 500 nM. The ^{35}S-labeled proteins were resolved on an 8% SDS polyacrylamide gel, and the dried gel was PhosphorImaged.

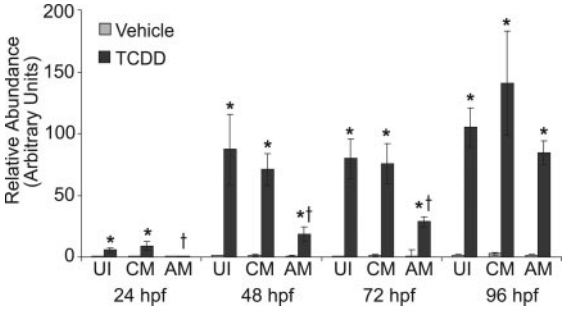

Fig. 7. Effect of the *zfarnt1*-MO on the time course of TCDD-induced zfCYP1A mRNA abundance in the zebrafish embryo. Quantitative real-time PCR was performed on cDNA using gene-specific primers for zfCYP1A and β-actin. Samples were run concurrently with standard curves derived from plasmid cDNA dilutions. Values obtained with the zfCYP1A primers were normalized to those obtained with β-actin primers to control for differences in loading and obtain relative values. RNA was extracted from pools of 15 embryos from each treatment group at each time (n = pool of 15 embryos) and reverse transcribed into cDNA. Values are mean ± S.E. of n = 4 pools. *, significant difference between TCDD and its respective vehicle control; †, significant difference between uninjected TCDD and TCDD + *zfarnt1*-MO ($p \leq 0.05$).

proteins are functioning with zfAHR2 to mediate zfCYP1A protein induction throughout the zebrafish embryo. Control morphant embryos exposed to TCDD show a similar staining pattern as uninjected embryos (data not shown).

There are a number of zfAHR2-mediated adverse responses to TCDD in the early embryo in addition to the transcriptional regulation of CYP1A (Prasch et al., 2003). Our next goal was to determine whether zfAHR2/zfARNT1 heterodimers are necessary for the manifestation of these toxic responses after TCDD exposure. Three characteristic endpoints of TCDD toxicity in fish early life stages—pericardial edema, reduction in peripheral blood flow, and craniofacial malformations—were examined in TCDD-exposed *zfarnt1* morphants. We found the *zfarnt1*-MO provided partial to complete protection against these endpoints, demonstrating that one or more forms of the zfARNT1 protein also play a role in mediating these effects of TCDD.

The effect of the *zfarnt1*-MO on TCDD-induced pericardial edema formation was examined at 72 and 96 hpf (Fig. 9). Significant formation of pericardial edema can be seen in TCDD-exposed uninjected and control-MO embryos at 72 hpf, indicating that these embryos are beginning to show the onset of TCDD toxicity (Fig. 9A). The edema fluid continued to accumulate in the pericardial sac of these embryos causing the area of the pericardium to increase in size to approximately twice that observed in vehicle-exposed embryos by 96 hpf. Strikingly, the *zfarnt1* morphants showed complete protection against the TCDD-induced increase in pericardial sac area. The pericardial sac in TCDD-treated *zfarnt1* morphants was similar to that seen in vehicle-exposed embryos at both 72 and 96 hpf. The protection that the *zfarnt1*-MO provides against TCDD-induced pericardial edema is depicted in photographs of representative embryos at 96 hpf (Fig. 9B). The TCDD-exposed *zfarnt1* morphants were observed through 144 hpf, and no pericardial or yolk sac edema ever developed (data not shown). A final point is that injection of the *zfarnt1*-MO alone did not cause the formation of any types of edema.

A second hallmark endpoint of TCDD developmental toxicity examined was peripheral blood flow (Fig. 10). Because peripheral blood flow is reduced after TCDD exposure earliest in the trunk, the number of red blood cells passing through an intersegmental vein in the posterior quarter of the trunk in 7.5 s was counted to determine red blood cell perfusion rates as an index of blood flow. At 72 hpf, intersegmental vein blood flow in TCDD-exposed uninjected and control morphants had decreased to approximately 65% of that observed in vehicle-exposed embryos. In contrast, no significant reduction was observed in the TCDD-exposed *zfarnt1* morphants. By 96 hpf intersegmental vein blood flow in TCDD-exposed uninjected embryos was more substantially decreased to 11% of that observed in vehicle-exposed embryos, and injection of the control-MO did not affect this decrease. A reduction in intersegmental vein blood flow was observed in the TCDD-exposed *zfarnt1* morphants at 96 hpf that was less severe than that observed in the other treatment groups, being reduced to approximately 56% of that observed in vehicle-exposed embryos. By 120 hpf, there was

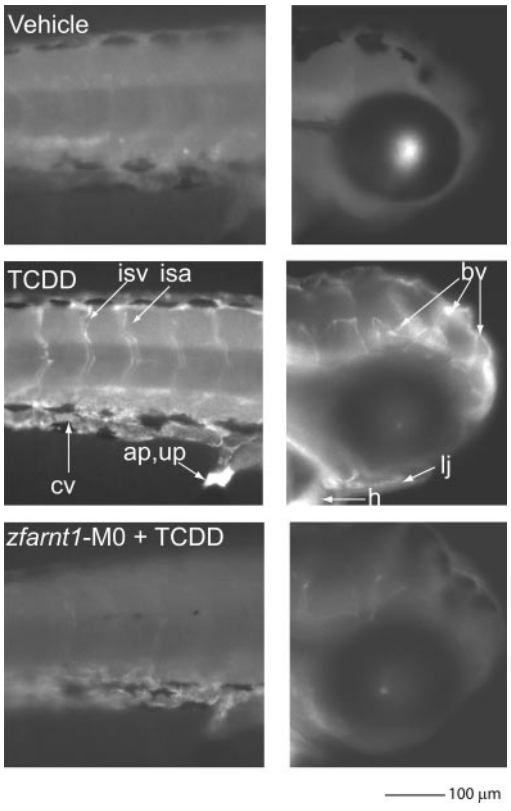

Fig. 8. Whole mount immunolocalization of zfCYP1A in vehicle and TCDD-exposed (0.4 ng/ml) uninjected embryos and TCDD-exposed *zfarnt1* morphants at 72 hpf using Mab1-12-3. Images on the left are lateral views of embryos taken posterior to the yolk extension, and images on the right are lateral views of the head taken anterior to the yolk sac. For each group, images are representative of 12 embryos from three distinct vehicle/TCDD exposure experiments. ap, anal pore; bv, brain vessels; cv, caudal vasculature; h, heart; isa, intersegmental artery; isv, intersegmental vein; lj, lower jaw; up, urinary pore. Scale bar, 100 μm.

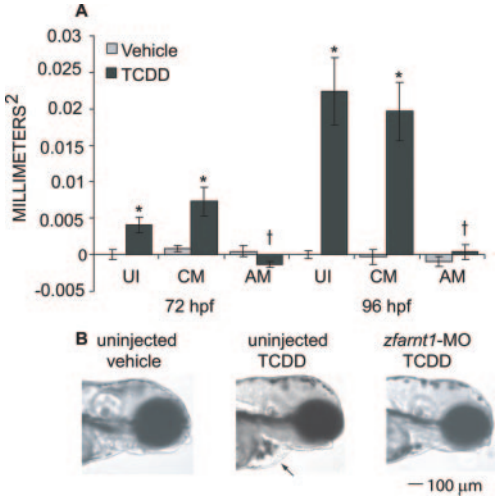

Fig. 9. Effect of the *zfarnt1*-MO on TCDD-induced increases in pericardial sac edema at 72 and 96 hpf in the zebrafish embryo. A, lateral views of embryos were photographed, and the area of the pericardial sac was quantitated at 72 and 96 hpf, respectively. The average area obtained for vehicle-exposed uninjected embryos was subtracted from the area values obtained for TCDD-exposed embryos in the other treatment groups to get a measure of the increase in pericardial area caused by edema. B, images are representative of the pericardial area observed in embryos exposed to vehicle, TCDD, or TCDD + *zfarnt2*-MO at 96 hpf. The arrow indicates the pericardial edema in uninjected TCDD-treated embryos. Values for edema quantitation are mean ± S.E. of $n = 12$. ∗, significant difference between TCDD (0.4 ng/ml) and its respective vehicle control ($p \leq 0.05$); †, significant difference between uninjected TCDD and TCDD + *zfarnt1*-MO. UI, uninjected; CM, control-MO; AM, *zfarnt1*-MO. Scale bar, 100 μm.

almost no blood flowing in the TCDD-exposed uninjected or control-MO-injected fish with the average blood flow being only 0.5% of that measured in vehicle-exposed embryos. Blood flow continued to be less severely reduced in the TCDD-exposed *zfarnt1* morphants and remained at approximately 57% of that observed in vehicle-exposed embryos.

Lower jaw growth in zebrafish is known to be impaired by TCDD exposure (Henry et al., 1997; Teraoka et al., 2002), and so the role of zfARNT1 proteins in mediating this specific TCDD response was evaluated (Fig. 11). The distance between the anterior edge of the lower jaw and the anterior edge of the eye was measured at 96 hpf, and this lower jaw-to-eye gap was used as an index of lower jaw growth. In the lateral view of vehicle-exposed embryos, the lower jaw can be seen extending near to the anterior edge of the eye (Fig. 11B), creating a lower jaw-to-eye gap that is quite small, about 30 μm (Fig. 11A). However, in TCDD-exposed embryos the growth of the lower jaw is reduced causing the lower jaw to be shorter and to extend to varying distances behind the anterior edge of the eye. Because the shorter jaw is farther behind the eye, a greater jaw-to-eye gap is obtained upon TCDD treatment.

In uninjected embryos TCDD causes growth of the lower jaw to be reduced so that the lower jaw-to-eye gap is almost 3 times greater than that seen in vehicle-exposed embryos (Fig. 11A). A similar effect of TCDD is evident in control morphant embryos. In contrast, the *zfarnt1* morphants exposed to TCDD showed a phenotype that was intermediate between that observed in vehicle and TCDD-exposed uninjected and control morphant embryos. Lower jaw growth was decreased in the TCDD-exposed *zfarnt1* morphants so that the jaw-to-eye gap was approximately 1.5-fold greater than that seen in vehicle-exposed embryos. However, this was still significantly less than the 3-fold increase in jaw-to-eye gap observed in uninjected and control morphant TCDD-exposed embryos, indicating that the reduction in lower jaw growth was less severe in the *zfarnt1* morphants.

Discussion

Characteristics of the zfARNT1 Proteins. In vitro assays were initially used to assess the functional characteristics of the zfARNT1 proteins. The DNA binding assay demonstrates that zfARNT1b and zfARNT1c are both able to function with zfAHR2 to form a strong complex with XRE-containing DNA, whereas zfARNT1a forms only a weak interaction. The results of the transactivation assay are consistent with the DNA binding results and demonstrate that both zfARNT1b and zfARNT1c are able to promote transactivation on the XRE-containing reporter construct when expressed with zfAHR2, whereas zfARNT1a is inactive. Overall, these results demonstrate that either zfARNT1b or zfARNT1c could be functioning in vivo as a dimerization partner for zfAHR2, whereas zfARNT1a probably plays no in vivo role in mediating TCDD toxicity. In addition, the results of the DNA binding and transactivation assays suggest that zfARNT1b and zfARNT1c may interact more strongly with zfAHR2 on XRE-containing promoter sequences than zfARNT2b.

In vitro characterization of the zfARNT1 splice variants also provides information about the functional domains of these proteins. The DNA binding results demonstrate that even though the N terminus containing the expected DNA binding domain is identical between the three zfARNT1 proteins, only zfARNT1b and zfARNT1c are able to interact with zfAHR2 to bind XRE-containing DNA. This finding is consistent with what has been observed for alternate splice variants of zebrafish *arnt2* (Tanguay et al., 2000) and rainbow trout *arnt* (Pollenz et al., 1996) where ARNT proteins with identical bHLH and PAS domains, but divergent C-terminal domains, showed differential ability to interact with DNA. C-terminal sequences are clearly important for the formation of protein/DNA complexes in vitro, although the identity of these sequences is unknown in zfARNT1.

Previous deletion studies have demonstrated that a potent transactivation domain localizes to the C-terminal end of ARNT proteins (Jain et al., 1994; Li et al., 1994; Sogawa et al., 1995; Nacela and Pollenz, 1999). It is noteworthy that both zfARNT1b and zfARNT1c have significant ability to

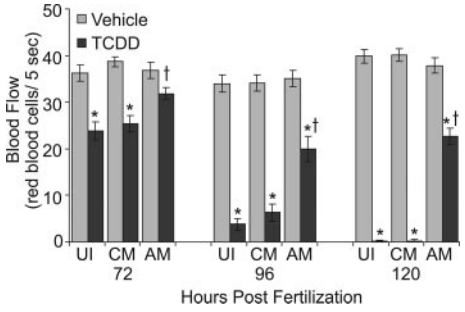

Fig. 10. Effect of the *zfarnt1*-MO on TCDD-induced reductions in peripheral blood flow at 72, 96, and 120 hpf in the zebrafish embryo. As an index of peripheral blood flow, red blood cell perfusion rates were determined in an intersegmental vein in the posterior quarter of the trunk. Values are mean ± S.E. of $n = 12$. UI, uninjected; CM, control-MO; AM, *zfarnt1*-MO. Other conditions as in Fig. 9 legend.

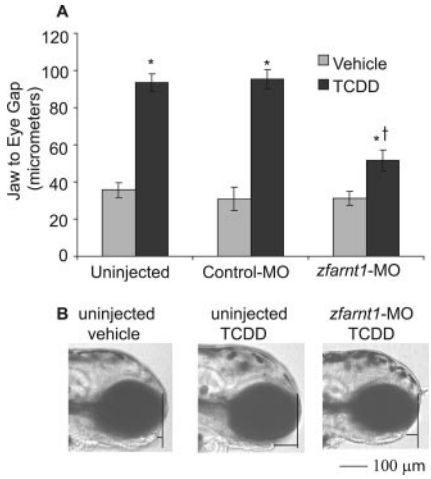

Fig. 11. Effect of the *zfarnt1*-MO on TCDD-induced increases in the lower jaw-to-eye gap. A, lateral views of the embryos were photographed and the lower jaw-to-eye gap was measured as an index of lower jaw growth at 96 hpf. B, representative lateral view photographs showing the length of the lower jaw in vehicle and TCDD-exposed (0.4 ng/ml) uninjected embryos and TCDD-exposed *zfarnt1* morphants are included. The way in which the jaw-to-eye distance was obtained is also depicted (B). First, a straight vertical line was drawn along the anterior most edge of the eye, and then a second straight horizontal line was drawn from the anterior most edge of the lower jaw to the intersection of the first vertical line. The length of this second horizontal line was used as the measure of lower jaw-to-eye gap. When the lower jaw protruded in front of the eye, the measure was a negative value, and if it remained behind the eye, it was given a positive value. Values are mean ± S.E. of $n = 12$. Scale bar, 100 μm. Other conditions as in Fig. 9 legend.

promote transactivation, even though zfARNT1b contains a truncated C-terminal domain compared with other ARNT proteins (Li et al., 1994; Pollenz et al., 1996; Tanguay et al., 2000). Further deletion studies need to be performed on the zfARNT1 proteins to determine the functional transactivation domains and the way in which these domains interact with transcription factors and coregulators to alter gene expression.

In Vivo Role of zfARNT1 Proteins in Mediating TCDD Developmental Toxicity. The experiments with the *zfarnt1*-MO clearly demonstrate that some form(s) of the zfARNT1 protein is required to dimerize with zfAHR2 in vivo to mediate the molecular and physiological endpoints of TCDD toxicity examined in this study. The protection that the *zfarnt1*-MO provides against the induction of both zfCYP1A mRNA and protein demonstrates that a zfARNT1 protein is essential for this change in gene expression to occur upon TCDD exposure. The zfCYP1A time-course study also provides information about the effectiveness of the morpholino and demonstrates that the *zfarnt1*-MO was no longer significantly blocking the zfAHR2 signaling pathway by 96 hpf. The *zfarnt1* morphants also show protection against three endpoints of TCDD toxicity—pericardial edema, reduced blood flow, and reduced lower jaw growth—demonstrating the essential role of a zfARNT1 protein in mediating toxicity. The results with the *zfarnt1*-MO demonstrate that one or more splice variant of the zfARNT1 protein mediates toxicity, but they do not provide information about the role that each splice variant of zfARNT1 is playing.

Differential Requirement of zfARNT1 and zfARNT2 in Mediating TCDD Toxicity. Although the zfARNT1b, zfARNT1c, and zfARNT2b proteins are all functional with zfAHR2 in vitro, the in vivo manipulation of these proteins described here and by Prasch et al. (2004b) has revealed that zfARNT1, not zfARNT2, proteins are an essential component of the zfAHR2 signaling pathway mediating the endpoints of TCDD toxicity assessed in these studies. The essential role of zfARNT1 proteins in mediating the TCDD-dependent block of regenerative growth has also been confirmed (Mathew et al., 2006). In addition, it has been demonstrated that knocking down expression of ARNT1 in mice provides protection against several endpoints of TCDD toxicity, demonstrating that in a mammalian species ARNT1 is also required for mediating many endpoints of AHR-dependent toxicity (Walisser et al., 2004).

One possible explanation for the differential requirement of the zfARNT proteins in mediating zfAHR2 signaling is that there are differential expression patterns of the proteins as has been observed in mammals (Hirose et al., 1996; Jain et al., 1998; Aitola and Pelto-Huikko, 2003). Quantitative real-time PCR of whole embryo tissue demonstrates that both zfARNT1a,b,c and zfARNT2 are expressed during the period of development when toxicity occurs, and zfARNT2 is a more abundant transcript. However, for zfARNT proteins to function with zfAHR2 in vivo to mediate TCDD toxicity, they must be coexpressed with the receptor in target tissues. Unfortunately, attempts at using in situ hybridization techniques to detect the tissue distribution of zfARNT1a,b,c mRNA in the early zebrafish embryo were unsuccessful, probably because of the low expression levels of these transcripts, and so it was not possible to compare the temporal and spatial expression pattern of zfARNT1a,b,c to that of zfAHR2 and zfARNT2 (Andreasen et al., 2002b).

It is also possible that zfARNT1 and zfARNT2 proteins are expressed in similar tissues, but zfARNT1 proteins are the preferred dimerization partner for zfAHR2 in vivo. The results from the in vitro assays suggest that zfARNT1b and zfARNT1c may interact more strongly with zfAHR2 on XRE-containing promoters and can promote a more robust level of transactivation on reporter constructs than zfARNT2b. Therefore, even if zfARNT1 and zfARNT2 proteins are coexpressed in the same tissues, zfARNT1 proteins may be the preferred dimerization partner for zfAHR2.

Mechanism of TCDD Toxicity. The results with the *zfahr2* and *zfarnt1* morpholinos clearly demonstrate that zfAHR2 and one or more forms of zfARNT1 are necessary to induce TCDD-dependent responses in zebrafish embryos. This provides insight into the mechanism by which activation of zfAHR2 by TCDD causes developmental toxicity in zebrafish. It has been hypothesized that the toxic effects of zfAHR2 activation could be independent of XRE binding and transcriptional activation and instead be because of interactions of zfAHR2 with other proteins (Prasch et al., 2004a). In mammals, the AHR has been shown to interact with a variety of other signaling pathways and proteins, including hormone, nuclear factor-κB, and hypoxia signaling pathways, and cell cycle proteins such as Rb (for review, see Carlson and Perdew, 2002). It as been speculated that cross-talk with other pathways may actually be the mechanism of TCDD toxicity. However, results from the current study demonstrate that both zfAHR2 and zfARNT1 are essential for the generation of developmental toxicity in zebrafish. Although it is possible that the zfAHR2/zfARNT1 heterodimer is uniquely capable of tethering other transcription factors leading to altered gene expression without binding to XRE sequences, it seems more likely that endpoints of toxicity are in fact dependent on XRE binding and alterations in gene expression caused by the zfAHR2/ARNT1 heterodimer. It has been shown that blocking induction of the zfCYP1A protein in zebrafish provides no protection against TCDD developmental toxicity (Carney et al., 2004), suggesting that altered regulation of other, currently unknown genes, may be important. However, until these genes and their roles in TCDD developmental toxicity have been clearly identified, mechanisms of cross-talk with other signaling pathways cannot be ruled out.

Role of zfARNT1 Proteins in Normal Development. Studies with *arnt1*$^{-/-}$ knockout mice lines clearly demonstrate that ARNT1 plays a role in normal mammalian development. *Arnt1*$^{-/-}$ knockout mice are not viable past embryonic day 10.5 and show defects in developmental angiogenesis (Kozak et al., 1997; Maltepe et al., 1997). The current study does not provide any insight into the role zfARNT1 proteins may play in mediating normal zebrafish development. The *zfarnt1* morphants were able to develop completely with no obvious gross abnormalities observed. Given the severity of the *arnt1*$^{-/-}$ mouse phenotype, it is surprising that the *zfarnt1* morphants developed normally. It is possible that our gross observations of the morphant embryos did not detect abnormalities that are more subtle. Alternate possibilities are that enough zfARNT1 protein remained present in the morpholino studies for normal physiological functions to be carried out or that there is functional

redundancy between zfARNT1 and other zebrafish ARNT proteins.

The results of this study provide further insight into the initial molecular signaling events that occur in zebrafish embryos upon exposure to TCDD. Although we now know that both zfAHR2 and some form of zfARNT1 are required for toxicity to develop, the way in which activation of these proteins by TCDD leads to toxicity is still unclear and remains a focus of future research. In addition, the way in which each of the zfARNT1 splice variants functions to mediate zfAHR2 signaling in vivo is also unknown. Finally, the role(s) that zfARNT1 proteins may play in dimerizing with other PAS proteins to mediate responses to other changing environmental or developmental conditions remains to be determined.

Acknowledgments

We thank Dorothy Nesbit for excellent technical assistance, Dr. John Stegeman (Woods Hole Oceanographic Institute) for the generous supply of the Mab1-12-3 antibody, and Sara Carney for helpful discussions on the manuscript. This article is contribution no. 366, Molecular and Environmental Toxicology Center, University of Wisconsin, Madison, WI.

References

Aitola MH and Pelto-Huikko MT (2003) Expression of Arnt and Arnt2 mRNA in developing murine tissues. *J Histochem Cytochem* **51:**41–54.

Andreasen EA, Hahn ME, Heideman W, Peterson RE, and Tanguay RL (2002a) The zebrafish (*Danio rerio*) aryl hydrocarbon receptor type 1 is a novel vertebrate receptor. *Mol Pharmacol* **62:**234–249.

Andreasen EA, Spitsbergen JM, Tanguay RL, Stegeman JJ, Heideman W, and Peterson RE (2002b) Tissue-specific expression of AHR2, ARNT2 and CYP1A in zebrafish embryos and larvae: effects of developmental stage and 2,3,7,8-tetrachlorodibenzo-p-dioxin exposure. *Toxicol Sci* **68:**403–419.

Carlson DB and Perdew GH (2002) A dynamic role for the Ah receptor in cell signaling? Insights from a diverse group of Ah receptor interacting proteins. *J Biochem Mol Toxicol* **16:**317–325.

Carney SA, Peterson RE, and Heideman W (2004) TCDD activation of the AHR/ARNT pathway causes developmental toxicity through CYP1A-independent mechanism in zebrafish. *Mol Pharmacol* **66:**512–521.

Cook PM, Robbins JA, Endicott DD, Lodge KB, Guiney PD, Walker MK, Zabel EW, and Peterson RE (2003) Effects of aryl hydrocarbon receptor-mediated early life stage toxicity on lake trout populations in Lake Ontario during the 20th century. *Environ Sci Technol* **37:**3864–3877.

Dong W, Teraoka H, Tsujimoto Y, Stegeman JJ, and Hiraga T (2004) Role of aryl hydrocarbon receptor in mesencephalic circulation failure and apoptosis in zebrafish embryos exposed to 2,3,7,8-tetrachlorodibenzo-p-dioxin. *Toxicol Sci* **77:**109–116.

Evans BR, Karchner SI, Franks DG, and Hahn ME (2005) Duplicate aryl hydrocarbon receptor repressor genes (ahrr1 and ahrr2) in the zebrafish *Danio rerio*: structure, function, evolution and AHR-dependent regulation in vivo. *Arch Biochem Biophys* **441:**151–167.

Fernandez-Salguero PM, Hilbert DM, Rudikoff S, Ward JM, and Gonzalez FJ (1996) Aryl-hydrocarbon receptor-deficient mice are resistant to 2,3,7,8-tetrachlorodibenzo-p-dioxin-induced toxicity. *Toxicol Appl Pharmacol* **140:**173–179.

Henry TR, Spitsbergen JM, Hornung MW, Abnet CC, and Peterson RE (1997) Early life stage toxicity of 2,3,7,8-tetrachlorodibenzo-p-dioxin in zebrafish (*Danio rerio*). *Toxicol Appl Pharmacol* **142:**56–68.

Hirose K, Morita M, Ema M, Mimura J, Hamada H, Fujii H, Saijo Y, Gotoh O, Sogawa K, and Fujii-Kuriyama Y (1996) cDNA cloning and tissue-specific expression of a novel basic helix-loop-helix/PAS factor (Arnt2) with close sequence similarity to the aryl hydrocarbon receptor nuclear translocator (Arnt). *Mol Cell Biol* **16:**1706–1713.

Jain S, Dolwick KM, Schmidt JV, and Bradfield CA (1994) Potent transactivation domains of the Ah receptor and the Ah receptor nuclear translocator map to their carboxyl termini. *J Biol Chem* **269:**31518–31524.

Jain S, Maltepe E, Lu MM, Simon C, and Bradfield CA (1998) Expression of ARNT, ARNT2, HIF1 alpha, HIF2 alpha and Ah receptor mRNAs in the developing mouse. *Mech Dev* **73:**117–123.

Karchner SI, Franks DG, and Hahn ME (2005) AHR1B, a new functional aryl hydrocarbon receptor in zebrafish: tandem arrangement of ahr1b and ahr2 genes. *Biochem J* **392:**153–161.

Kozak KR, Abbott B, and Hankinson O (1997) ARNT-deficient mice and placental differentiation. *Dev Biol* **191:**297–305.

Li H, Dong L, and Whitlock JP Jr (1994) Transcriptional activation function of the mouse Ah receptor nuclear translocator. *J Biol Chem* **269:**28098–28105.

Maltepe E, Schmidt JV, Baunoch D, Bradfield CA, and Simon MC (1997) Abnormal angiogenesis and responses to glucose and oxygen deprivation in mice lacking the protein ARNT. *Nature (Lond)* **386:**403–407.

Mathew L, Andreasen EA, and Tanguay RL (2006) Aryl hydrocarbon receptor activation inhibits regenerative growth. *Mol Pharmacol* **69:**257–265.

Mimura J, Yamashita K, Nakamura K, Morita M, Takagi TN, Nakao K, Ema M, Sogawa K, Yasuda M, Katsuki M, and Fujii-Kuriyama Y (1997) Loss of teratogenic response to 2,3,7,8-tetrachlorodibenzo-p-dioxin (TCDD) in mice lacking the Ah (dioxin) receptor. *Genes Cells* **2:**645–654.

Nasevicius A and Ekker SC (2000) Effective targeted gene 'knockdown' in zebrafish. *Nat Genet* **26:**216–220.

Nacela B and Pollenz RS (1999), Functional analysis of activation and repression domains of the rainbow trout aryl hydrocarbon receptor nuclear translocator (rtARNT) protein isoforms. *Biochem Pharmacol* **57:**1177–1190.

Park SS, Miller H, Klotz AV, Kloepper-Sams PJ, Stegeman JJ, and Gelboin HV (1986) Monoclonal antibodies to liver microsomal cytochrome P-450 E of the marine fish *Stenotomus chrysops* (scup): cross reactivity with 3 methylcholanthrene induced rat cytochrome P-450. *Arch Biochem Biophys* **249:**339–350.

Peterson RE, Theobald HM, and Kimmel GL (1993) Developmental and reproductive toxicity of dioxins and related compounds: cross-species comparisons. *Crit Rev Toxicol* **23:**283–335.

Pollenz RS, Sullivan HR, Holmes J, Necela B, and Peterson RE (1996) Isolation and expression of cDNAs from rainbow trout (*Oncorhynchus mykiss*) that encode two novel basic helix-loop-Helix/PER-ARNT-SIM (bHLH/PAS) proteins with distinct functions in the presence of the aryl hydrocarbon receptor. Evidence for alternative mRNA splicing and dominant negative activity in the bHLH/PAS family. *J Biol Chem* **271:**30886–30896.

Prasch AL, Andreasen EA, Peterson RE, and Heideman W (2004a) Interactions between 2,3,7,8-tetrachlorodibenzo-p-dioxin (TCDD) and hypoxia signaling pathways in zebrafish: hypoxia decreases responses to TCDD in zebrafish embryos. *Toxicol Sci* **78:**68–77.

Prasch AL, Heideman W, and Peterson RE (2004b) ARNT2 is not required for TCDD developmental toxicity in zebrafish. *Toxicol Sci* **82:**250–258.

Prasch AL, Teraoka H, Carney SA, Dong W, Hiraga W, Stegeman JJ, Heideman W, and Peterson RE (2003) Aryl hydrocarbon receptor 2 mediates 2,3,7,8-tetrachlorodibenzo-p-dioxin developmental toxicity in zebrafish. *Toxicol Sci* **76:**138–150.

Schmidt JV and Bradfield CA (1996) Ah receptor signaling pathways. *Annu Rev Cell Dev Biol* **12:**55–89.

Sogawa K, Iwabuchi K, Abe H, and Fujii-Kuriyama Y (1995) Transcriptional activation domains of the Ah receptor and Ah receptor nuclear translocator. *J Cancer Res Clin Oncol* **121:**612–620.

Tanguay RL, Abnet CC, Heideman W, and Peterson RE (1999) Cloning and characterization of the zebrafish (*Danio rerio*) aryl hydrocarbon receptor. *Biochim Biophys Acta* **1444:**35–48.

Tanguay RL, Andreasen E, Heideman W, and Peterson RE (2000) Identification and expression of alternatively spliced aryl hydrocarbon nuclear translocator 2 (ARNT2) cDNAs from zebrafish with distinct functions. *Biochim Biophys Acta* **1494:**117–128.

Tanguay RL, Andreasen EA, Walker MK, and Peterson R (2003) Dioxin toxicity and aryl hydrocarbon receptor signaling in fish, in *Dioxins and Health*, 2nd ed (Schecter A and Gasiewicz TA eds) pp 603–628, John Wiley & Sons, Inc., New York.

Teraoka H, Dong W, Ogawa S, Tsukiyama S, Okuhara Y, Niiyama M, Ueno N, Peterson RE, and Hiraga T (2002) 2,3,7,8-Tetrachlorodibenzo-p-dioxin toxicity in the zebrafish embryo: altered regional blood flow and impaired lower jaw development. *Toxicol Sci* **65:**192–199.

Teraoka H, Dong W, Tsujimoto Y, Iwasa H, Endoh D, Ueno N, Stegeman JJ, Peterson RE, and Hiraga T (2003) Induction of cytochrome P450 1A is required for circulation failure and edema by 2,3,7,8-tetrachlorodibenzo-p-dioxin in zebrafish. *Biochem Biophys Res Commun* **304:**223–228.

Walisser JA, Bunger MK, Glover E, Harstad EB, and Bradfield CA (2004) Patent ductus venosus and dioxin resistance in mice harboring a hypomorphic Arnt allele. *J Biol Chem* **279:**16326–16331.

Wang WD, Wu JC, Hsu HJ, Kon ZL, and Hu CH (2000) Overexpression of a zebrafish ARNT2-like factor represses CYP1A transcription in ZLE cells. *Mar Biotech* **2:**376–386.

Wentworth JN, Buzzeo R, and Pollenz RS (2004) Functional characterization of aryl hydrocarbon receptor (zfAHR2) localization and degradation in zebrafish (*Danio rerio*). *Biochem Pharmacol* **67:**1363–1372.

Westerfield M (1995) *The Zebrafish Book*, University of Oregon Press, Eugene, OR.

Address correspondence to: Dr. Richard E. Peterson, School of Pharmacy, University of Wisconsin, 777 Highland Ave., Madison, WI 53705-2222. E-mail: repeterson@pharmacy.wisc.edu